

Contact fracture resistance of physically and chemically tempered glass plates: a theoretical model

B. R. Lawn & D. B. Marshall

School of Physics, University of New South Wales, Kensington, Australia

Manuscript received 23 April 1976

A fracture analysis of contact-induced failure in tempered glass plate is presented. The analysis is based on a model system in which a surface-initiated crack of appropriately simple geometry is driven through a well defined stress field in the plate. The general field is taken to consist of three main components: a residual field, due to the tempering process, either physical or chemical, for which idealised stress profiles across the plate (basically, outer compression, inner tension) are assumed; an indentation field, either line-contact or point-contact type, corresponding to straight or penny-like crack geometries; a flexural field, due to plate bending. Of these components, only the first two are dealt with explicitly in this study, although the generality of the approach is emphasised. The onset of plate failure is identified with an instability in the crack propagation, which, for the combined indentation/residual field, is associated with a critical contact load ("activated failure"); in the special case of a (remnant) crack for which the indentation field is zero, the instability is associated with a critical intensity of inner tension in the plate ("spontaneous failure").

In the first part of the calculation the simplistic case of a straight crack of infinite extent along its front is considered in detail. This configuration, although somewhat unrealistic, establishes the mechanics of the failure process without complication. In the latter part the treatment is generalised to include the more practical case of penny-like cracks, at some expense in mathematical rigour. The theory leads to "universal" equilibrium relations for crack dimension in terms of indenter load, from which the instability conditions are derived.

A feature of the resulting equations for the critical indentation load to failure is their simplicity of form, particularly in the limit of "severe tempering". The key parameters in these equations are those relating to the tempering process, notably the intensity and spatial extent of the residual field, and to the nature of the indenter/specimen contact; material constants are of secondary importance, disappearing altogether from the limiting equations, and flaw characteristics do not enter at all. Plates characterised by typical degrees of tempering are predicted to fail, to good approximation, within the compass of this limiting behaviour. Notwithstanding

an inability in our present formulation to determine proportionality constants in the critical equations to much better than an order of magnitude, the theoretical model should provide a sound basis for predetermining optimum strength conditions in potentially deleterious contact situations.

Ever since Griffith's classic study of the rupture of glass⁽¹⁾ it has been recognised that the ubiquitous presence of surface flaws (of effective length $\lesssim 10 \mu\text{m}$ typically) reduces the potential stress-bearing capacity of engineering brittle solids by at least two orders of magnitude. Various attempts have been made to achieve tensile strengths closer to the ultimate limit determined by intrinsic cohesive forces by producing materials free of flaws, for example by etching the surfaces; however, the question of durability under subsequent hostile service conditions generally renders this approach impractical. By far the most effective way of strengthening glasses (and to a lesser extent other, crystalline, ceramics) is to generate a state of compression in their surfaces.⁽²⁻⁵⁾ This may be done either physically, by thermally quenching glass plate from just below its softening point, or chemically, by suitably modifying the atomic structure of the surface regions of the glass (notably by ion exchange). Both procedures introduce residual compressive stresses which inhibit the growth of incipient surface flaws to such an extent that the applied tensile loading necessary to achieve critical conditions for fracture may be raised significantly toward the theoretical limit. Chemical strengthening, as compared to its physical counterpart, appears capable of producing the higher intensity of stress within the surface compression layer, but only at the expense of spatial extent (e.g. $\approx 1000 \text{ MPa}$ over a layer thickness $\approx 0.1 \text{ mm}$, as compared to $\approx 100 \text{ MPa}$ over $\approx 1 \text{ mm}$).

The net residual force on a strengthened glass plate must, of course, be zero. Thus the outer compression must be balanced by an inner tension, so that a crack, once it does penetrate the protective surface layer, tends to propagate catastrophically. If the degree of tempering is sufficiently high, such propagation may occur spontaneously, i.e. in the absence of any

externally applied load. It is this property which makes it almost impossible to cut or drill glass plate in the tempered state. The accelerating crack tends to bifurcate repeatedly, its surfaces remaining more or less normal to, and confined within, the outer boundaries of the plate, until the entire plate has fragmented in a characteristic craze pattern.

In practice, tempered glass plates subjected to external loading fail in one of two basic modes.^(6,7) With the first mode, the plate undergoes flexure, thereby inducing compressive stresses in the loaded face, tensile stresses in the opposite face. (For dynamic loading, any subsequent vibration naturally causes a reversal of these stresses.) Full scale fracture initiates at some dominant flaw remote from the contact area, and the strengthening effect arises simply from the need to overcome the residual closure stresses acting across this flaw before a net tension can become manifest. In this situation the strength of the tempered plate is found to be, in the limit of flaws small compared with the spatial extent of the outer protective layer, closely equal to the strength of the untreated plate plus the magnitude of the surface residual compression. It is clear that in any complete description of the strength properties one needs to take into account the circumstances leading to the presence of the dominant flaw: the issues of specimen history, and thence of flaw statistics, are directly relevant here.

With the second mode of failure, the contact stresses (alternatively termed "indentation", or "bearing", stresses) dominate the overall applied field. Fracture then initiates in the near-contact zone, and develops geometrically in a characteristic pattern which reflects the nature of the indenter/plate contact. The best-known example of a contact fracture is the Hertzian cone crack, produced by a hard sphere. With less regular indenters the fracture patterns become more difficult to characterise; moreover, the number of variants would appear to be unlimited. It is because of this apparent diversity in fracture geometry, coupled with the complexity of the general indentation field through which the cracks propagate, that our understanding of the mechanisms of contact failure has been slow in evolving. Nevertheless, this mode is potentially the more dangerous of the two: as pointed out by Glathart & Preston,⁽⁷⁾ a thermally strengthened plate may withstand the drop of a massive steel ball from the top of a building, yet collapse like a bubble from the impact of a little steel dart released from a height of ≈ 100 mm. Intuitively, one might expect a variety of extrinsic variables, notably the intensity and spatial extent of the residual field in the tempered plate, the indenter/plate contact stress distribution, flaw parameters, etc., and intrinsic variables, such as toughness, hardness and stiffness, to enter the problem. Few serious attempts, even of a preliminary or empirical nature, have been made to evaluate the role of any of these variables in the indentation-induced failure of tempered glass objects.^(5,7)

However, recent developments in the theory of indentation fracture phenomena⁽⁸⁻¹⁰⁾ reveal features

of common simplicity in the general growth patterns, from which emerge the foundations for a detailed failure analysis. In particular, the indentation cracks, while certainly determined by the nature of the starting flaws in their initiation stages, tend in their "well developed" form to propagate independently of their origin in accordance with certain universal relations between applied load and crack dimension. It is the prime intent of this paper to formulate an appropriate failure analysis along these lines. We concentrate on situations where the contact stresses are completely dominant, mindful of the increasing relative importance of flexural stresses with diminishing plate thickness.⁽⁷⁾ Whereas others have addressed the problem of fragmentation once catastrophic fracture has begun,^(11,12) our treatment considers only the critical conditions for the onset of failure; for it is surely this second aspect which must provide the basis for optimum preventative design. The procedure involves setting up a somewhat simplistic model of a static indentation fracture process, applying the principles of Griffith-Irwin fracture mechanics to the model,⁽¹³⁾ and then attempting to generalise the results. The emergent critical equations, which in the limit of severe tempering reduce to strikingly simple form, are found to have interesting, perhaps surprising, implications concerning the parameters which control resistance to contact failure.

The residual stress field—basic fracture mechanics relations

STRESS INTENSITY FACTORS FOR STRAIGHT CRACKS IN INHOMOGENEOUS RESIDUAL FIELDS

We need first to specify the residual stress profiles in tempered plates free of external loading, and thence to establish suitable parameters for representing the capacity of surface cracks to extend within such plates. Accordingly, we use the residual field equations to evaluate the stress intensity factors, which measure the intensity of the local stress field about the crack tips (hence the driving force for the cracks as individual mechanical entities) and which may readily be incorporated into fundamental fracture criteria.⁽¹³⁾ What happens when the plates are loaded will be taken up later.

Coordinates for the envisaged cracked plate system are shown in Figure 1. Along the surface normal OZ

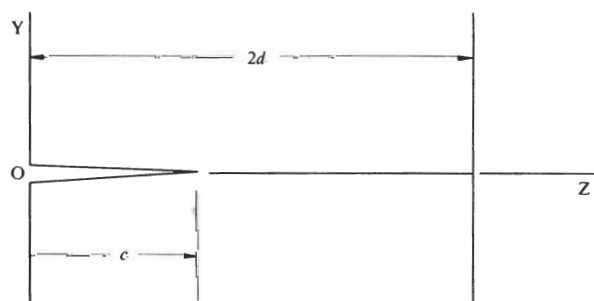


Figure 1. Coordinates for straight crack system in tempered plate

the plate has thickness $2d$, and within the surface plane OXY the dimensions are infinite. In this description the residual stress field assumes the single-variable functional form $\sigma = \sigma(z)$. The simplest fracture configuration conformant with this field is that of a straight crack of infinite extent along OX (say), with its mouth at $z = 0$ and its tip at $z = c$; then the front of the crack coincides with a stress contour at all points of its prospective extension through the field, and the configuration is thus essentially two dimensional. For this special case a standard formula is available for the stress intensity factor:^(13, 14)

$$K(c) = m_E \left\{ 2(c/\pi)^{\frac{1}{2}} \int_0^c [\sigma(z)/(c^2 - z^2)^{\frac{1}{2}}] dz \right\}, \quad (0 \leq c \leq 2d). \quad (1)$$

Here m_E is a dimensionless factor which takes into account "edge effects"; in a homogeneous field, for instance, m_E incorporates a factor 1.12 to account for the free surface at $z = 0$, and a factor $(4d/\pi c) \tan(\pi c/4d)$ to account for the free surface at $z = 2d$.^(13, 14) However, for the present system, in which the field is necessarily far from homogeneous, the approximation $m_E \approx 1$ will suffice where any absolute evaluation is required.

Physically tempered plate

Detailed studies of the process of thermal tempering in glass plates^(15, 16) indicate the distribution of residual (biaxial) stresses acting in the OXY plane to be closely parabolic across the thickness, with maximum compression at the free surfaces and maximum tension at the centre. Figure 2 shows the stress profile.

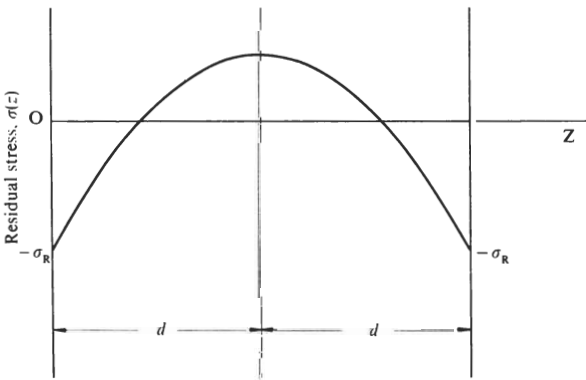


Figure 2. Residual stress profile for physically tempered plate

Defining σ_R as the magnitude of the surface compression, the boundary conditions $\sigma(0) = -\sigma_R = \sigma(2d)$, along with the requirement that the total force across the section OXZ (area under curve of Figure 2, representing section width unity along OX) be zero, i.e.

$$\int_0^{2d} \sigma(z) dz = 0,$$

determine the parabolic equation;

$$\sigma(z) = -\sigma_R(1 - 3z/d + 3z^2/2d^2), \quad (0 \leq z \leq 2d). \quad (2)$$

For this distribution we have $\sigma(d) = 0.5 \sigma_R$, i.e. the central tension is of magnitude one half that of the surface compression. Further, $\sigma(z) = 0$ at $z/d = 0.423, 1.577$, so that each outer compression layer extends into about one fifth the total thickness of the plate. The two parameters σ_R and d uniquely determine the field, within the approximation of the parabolic representation of Equation (2).

Let us now insert Equation (2) into Equation (1) and integrate over the crack length to obtain the "residual stress intensity factor",

$$K_R(c) = m_E \left\{ -\sigma_R(\pi c)^{\frac{1}{2}} (1 - 6c/\pi d + 3c^2/4d^2) \right\}, \quad (0 \leq c \leq 2d). \quad (3)$$

This expression takes on a particularly convenient parametric form if rewritten in terms of reduced variables,

$$K_R(c/d) = -M(c/d) \sigma_R(\pi d)^{\frac{1}{2}}, \quad (4)$$

where M is a dimensionless factor,

$$M(c/d) = m_E \left\{ (c/d)^{\frac{1}{2}} (1 - 6c/\pi d + 3c^2/4d^2) \right\}. \quad (5)$$

This factor is seen from Equation (4) to represent a normalised stress intensity factor for physically tempered plate; it is accordingly plotted in Figure 3, in the approximation $m_E \approx 1$. We may note that increasing the degree of tempering, as determined by the quantity $\sigma_R(\pi d)^{\frac{1}{2}}$, has the effect of increasing the absolute scale of $K_R(c)$.

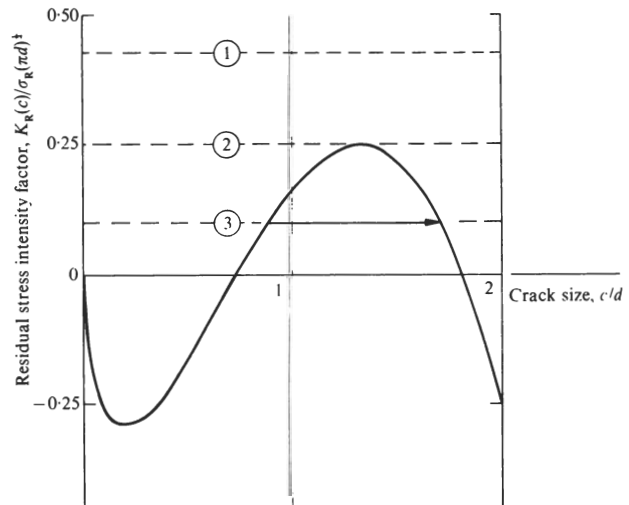


Figure 3. Normalised plot of stress intensity factor as function of crack size for physically tempered plate, zero external loading. Horizontal broken lines represent condition $K_I = \text{const.}$ at increasing degrees of tempering: arrow indicates crack instability

It is seen in Figure 3 that $K_R < 0$ for cracks in the size ranges $0 < c/d < 0.737$ and $1.810 < c/d < 2$; in these ranges cracks experience a net closure force. Conversely, $K_R > 0$ in the range $0.737 < c/d < 1.810$; here,

cracks experience a net opening force. However, little more than this may be deduced about the mechanics of crack growth until we introduce a specific fracture criterion.

Chemically tempered plate

The stress profile for chemically tempered glass plate is similar to that for physically tempered plate in that zones of surface compression are compensated by a zone of central tension. However, significant differences are also evident. The spatial extent of the compression layers is no longer determined by the thickness of the plate, but rather by some dimension δ characteristic of the chemical strengthening process (e.g. diffusion depth in ion-exchange process); typically, $\delta \ll d$. Figure 4 illustrates the approximate form

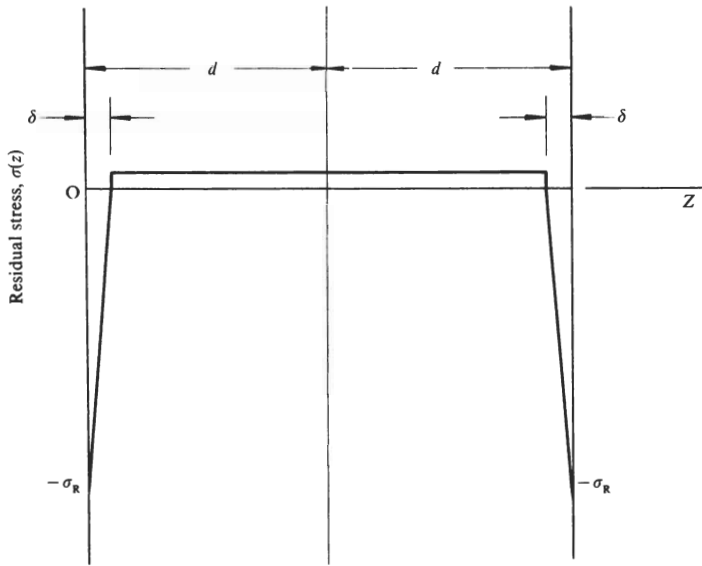


Figure 4. Residual stress profile for chemically tempered plate

of the profile.^(2-4, 17) Within these two outer zones the distribution is taken to be linear: in the "near surface" zone (corresponding to surface from which crack originates) the boundary conditions are $\sigma(0) = -\sigma_R$ and $\sigma(\delta) = 0$, so that the required linear equation is

$$\sigma(z) = -\sigma_R(1 - z/\delta), \quad (0 \leq z \leq \delta); \quad (6a)$$

in the "far surface" zone, $\sigma(2d) = -\sigma_R$ and $\sigma(2d - \delta) = 0$, giving

$$\sigma(z) = -\sigma_R(1 - 2d/\delta + z/\delta), \quad (2d - \delta \leq z \leq 2d). \quad (6c)$$

Within the inner zone, unaffected by direct chemical interactions, the stress level is taken to be constant: invoking the requirement that the area under the curve in Figure 4 be zero, we evaluate, in the approximation $\delta \ll d$,

$$\sigma(z) \approx \sigma_R(\delta/2d) = \text{const.}, \quad (\delta \leq z \leq 2d - \delta). \quad (6b)$$

In this case three parameters, σ_R , δ , and d , are needed to determine the field uniquely.

Substitution of Equations (6) into Equation (1) then

leads to the following expressions for the stress intensity factor:

$$K_R(c/\delta, \delta/d) = -M(c/\delta, \delta/d) \sigma_R(\pi\delta)^{\frac{1}{2}} \quad (7)$$

where M for each stress zone is

$$M(c/\delta, \delta/d) = m_E(c/\delta)^{\frac{1}{2}}(1 - 2c/\pi\delta), \quad (0 \leq c \leq \delta); \quad (8a)$$

$$= m_E(c/\delta)^{\frac{1}{2}}\{(1 + \delta/2d)(2/\pi) \sin^{-1}(\delta/c) - (2c/\pi\delta)[1 - (1 - \delta^2/c^2)^{\frac{1}{2}}] - \delta/2d\}, \quad (\delta \leq c \leq 2d - \delta); \quad (8b)$$

$$= m_E(c/\delta)^{\frac{1}{2}}\{(1 + \delta/2d)(2/\pi) \sin^{-1}(\delta/c) - (2c/\pi\delta)[1 - (1 - \delta^2/c^2)^{\frac{1}{2}}] - (\delta/\pi d) \sin^{-1}[(2d - \delta)/c] + (1 - 2d/\delta)(1 - (2/\pi) \sin^{-1}[(2d - \delta)/c]) + (2c/\pi\delta)(1 - [(2d - \delta)/c]^2)^{\frac{1}{2}}\}, \quad (2d - \delta \leq c \leq 2d). \quad (8c)$$

The stress intensity function of Equation (7), in conjunction with Equations (8), is plotted in normalised form in Figure 5, once more in the approximation $m_E \approx 1$, for two values of δ/d . It is noted that the plate thickness enters the fracture mechanics (by virtue of its role in determining the level of central tension) only after the crack has escaped the near compression zone.

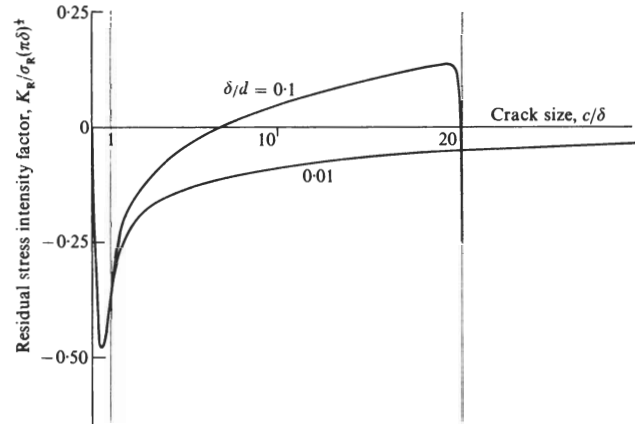


Figure 5. Normalised plot of stress intensity factor as function of crack size for chemically tempered plate, zero external loading. Curves shown for two values of δ/d : note invariance of plot in near compression zone $0 \leq c \leq \delta$

Thus, while it is the near zone quantity $\sigma_R(\pi\delta)^{\frac{1}{2}}$ which appears to define the degree of tempering (by establishing the absolute scale of $K_R(c)$ in Figure 5) most adequately for chemically treated plate, the thickness largely determines the crack size domains within which net closure or opening forces operate: e.g. for the limiting case $\delta \ll d$ in Equations (8), we find $K_R < 0$ in the ranges $0 < c/d < 0.637$ and $2 - \delta/d \leq c/d < 2$, and $K_R > 0$ in the range $0.637 < c/d < 2 - \delta/d$.

FRACTURE CRITERIA AND SPONTANEOUS CRACK PROPAGATION

Equilibrium and kinetic fracture

To be able to make quantitative predictions of fracture behaviour, suitable criteria have to be introduced into

the description. In a general treatment, one must specify criteria for both initiation and propagation stages.⁽¹³⁾ Thus far we have considered the effective driving force for a propagating crack of length c without making any comment as to the origin of the fracture. In practice, the most common origin is via mechanical damage: scratching, cutting, drilling, particle impact, etc. are all capable of initiating penetrant cracks. Certain chemical and thermal processes may also act as crack initiating sources. Such cracks may either nucleate from a suitable pre-existing flaw in the vicinity of the damage zone, or, in cases where the stress is locally concentrated at a level approaching the theoretical limit, be nucleated by the damage process itself. Once a given crack has grown beyond the immediate zone of influence of the nucleating forces it is said to be well developed. In this picture one may view the overall nucleation and formation stages of growth as an initial, restraining perturbation on the far field of the applied loading through which the well developed crack propagates; that is, a crack of zero dimension must first overcome an energy barrier. For instance, Hertzian cone cracks are produced only upon exceeding a critical indentation load:⁽⁶⁾ beyond this load, however, the fully developed cones propagate independently of the critical conditions. In this work we shall assume that the energy barrier to initiation is negligible, which is reasonable if the well developed crack thereby formed is small compared with that needed to cause total plate failure. The commonplace observation of intact tempered glass objects (notably automobile wind-screens) containing clearly visible surface cracks (remnant from some earlier damage event) will be taken as sufficient justification for this assumption at present.

It then becomes necessary only to specify conditions for the propagation of well-developed cracks. At the outset, we must distinguish between equilibrium and kinetic conditions. With equilibrium cracks, the net driving force just balances the intrinsic (surface tension) resisting force, corresponding to a stationary value in the total energy of the crack system (Griffith condition). In terms of stress intensity factor notation, this condition may be written⁽¹³⁾

$$K = K_c = [2\Gamma E/(1-\nu^2)]^{\frac{1}{2}} \quad (9)$$

with the critical value K_c uniquely determined by the material constants Γ , the fracture surface energy, E , the Young's modulus, and ν , the Poisson's ratio, of the plate. At $K > K_c$ the crack accelerates dynamically (terminal velocity $\approx 1.5 \text{ kms}^{-1}$ in glass), while at $K < K_c$ the crack tends to close up (but rarely completely, thus explaining the visibility of remnant interfaces). Equilibrium conditions tend to prevail in inert atmospheres, or at low temperatures and rapid loading rates.

With kinetic cracks, the net driving force falls below that required to satisfy Equation (9), but is nevertheless large enough to activate subcritical mechanisms of crack growth. Since much mechanisms are gener-

ally rate-dependent, the appropriate criterion involves a crack velocity,

$$v_c = v_c(K), \quad (0 \leq K < K_c), \quad (10)$$

where $v_c(K)$ is a positive, monotonically increasing function (typically, up to $\approx 1 \text{ mm s}^{-1}$). Kinetic growth in glass is primarily due to chemical interactions with environmental water molecules at the crack tip.⁽¹⁸⁾

Spontaneous growth of remnant cracks

We are now in a position to make some quantitative predictions about crack behaviour in tempered plate. Consistent with the straight crack analysis developed thus far, it is taken that the external loading responsible for initiating the fracture is removed prior to attaining the level necessary to take the plate to total failure. Then if the remnant crack were subsequently to satisfy the dynamic condition $K_R > K_c$ through the agency of incremental driving forces (e.g. mechanical or thermal shocks, chemically induced subcritical growth), the situation would be ripe for crack bifurcation, thence spontaneous breakup. To see how the condition for spontaneous propagation may be influenced by the degree of tempering, we refer to the special case of physically strengthened plate, Figure 3. Here the sequence of horizontal broken lines represents the condition $K_c = \text{const.}$ at successively higher levels of temper. If the appropriate value of K_c corresponds to line 1 for a given plate, then the requirement for dynamic growth clearly can not be satisfied at any crack dimension. (Under these conditions it should be perfectly safe to cut or drill the plate, provided such an operation does not itself substantially contribute to the net driving force on any penetrant fissure.) On the other hand, if line 3 is appropriate, a crack penetrating to the second (unstable) branch of the curve in Figure 3 will extend spontaneously from that branch toward the third (stable) branch, as indicated by the arrow. Thus line 2 represents our critical condition for spontaneous propagation, which may be written

$$K_c = [K_R(c)]_{\text{max}} = K_R(1.325 d) = 0.246 \sigma_R(\pi d)^{\frac{1}{2}},$$

or, approximately,

$$\sigma_R(\pi d)^{\frac{1}{2}} \approx 4K_c. \quad (11)$$

Physically, this result indicates that the degree of tempering needs to be at least four times as great as the intrinsic resistance to crack growth afforded by the material if spontaneous failure is to be at all possible. For typical silicate glasses, $K_c \approx 5 \times 10^5 \text{ N m}^{-3/2}$,⁽¹⁹⁾ with a plate half thickness $d \approx 3 \text{ mm}$, Equation (11) gives $\sigma_R \approx 21 \text{ MPa}$, a stress level easily attained in most thermal tempering setups. Of course, because of our earlier approximation $m_E \approx 1$ in plotting the curve in Figure 3, absolute values should be regarded with some caution.

An analogous treatment for chemically strengthened plate, Figure 5, gives

$$K_c = [K_R(c)]_{\text{max}} = K_R(2d - \delta) = 0.482 \sigma_R(\pi \delta)^{\frac{1}{2}} (\delta/d)^{\frac{1}{2}}$$

in the limit $\delta \ll d$ in Equations (8). The prerequisite for spontaneous growth thus becomes

$$\sigma_R(\pi\delta)^{\frac{1}{2}} \approx 2K_c(d/\delta)^{\frac{1}{2}} \quad (12)$$

Idealised straight crack model for indentation induced failure

STRESS INTENSITY FACTORS FOR STRAIGHT CRACKS IN INDENTATION-LOADED TEMPERED PLATE

The straight crack calculation above provides an indication of the prospective behaviour of tempered plate containing a fissure remnant from some past contact (or other) damage event. However, most failures occur during, not after, any such event. We must now incorporate details of the contact driving force for the fracture into our description. Here, the additive property of stress intensity factors⁽¹³⁾ allows for a convenient extension of the analysis developed thus far.

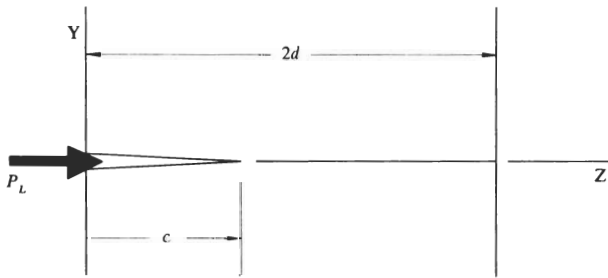


Figure 6. Coordinates for indentation-driven straight crack system in tempered plate

A suitably modified fracture system is shown in Figure 6. Consistent with the original straight crack picture, we characterise the contact interaction by the normally applied load P_L per unit length along OX. Prior to fracture the attendant indentation field contains a strong component of tension across the prospective separation plane,⁽¹⁰⁾ and it is this tension which drives the formative cracks. Once developed, the crack is driven by essentially localised, mouth loading forces, representing effective “wedging” components of the applied loading. Stress intensity factors for well developed indentation cracks in homogeneous plates have been derived elsewhere:^{(20, 21)†} the general result for straight cracks is expressible in terms of the “bearing stress intensity factor”

$$K_B(c) = \chi P_L/c^{\frac{1}{2}} = \chi P/Lc^{\frac{1}{2}} \quad (13)$$

where $P = P_L L$ is the total load on a (real) finite indenter of length $L (\geq d)$. (Recall that the crack of Figure 1 was taken to be of infinite extent along OX.) In this equation, χ , like m_E in Equation (1), is a dimensionless contact “constant” which incorporates several uncertain geometrical factors, such as indenter shape, indenter/specimen friction, etc.⁽²⁰⁾

For a straight crack in the combined fields of the bearing and residual stresses, we accordingly obtain the general stress intensity factor equation

$$K(\mathcal{C}) = K_B(\mathcal{C}) + K_R(\mathcal{C}) = \chi P/L\lambda^{\frac{1}{2}} \mathcal{C}^{\frac{1}{2}} - M(\mathcal{C}) \sigma_R(\pi\lambda)^{\frac{1}{2}}, \quad (14)$$

with $\mathcal{C} = c/\lambda$ a reduced crack size, λ being a characteristic residual field dimension (for example, d in Equation (4) for physically tempered plate, δ in Equation (7) for chemically tempered plate). This equation, taken in conjunction with an appropriate fracture criterion, provides the starting point for a detailed fracture mechanics analysis.

EQUILIBRIUM CRACK RELATIONS AND CRITICAL INDENTATION CONDITIONS

Now let us suppose that the indentation-driven crack evolves under conditions of equilibrium growth. Then Equation (9) may be combined with Equation (14) to obtain an explicit relation for the applied load as a function of crack size,

$$\chi P/K_c L\lambda^{\frac{1}{2}} = \mathcal{C}^{\frac{1}{2}} \{1 + M(\mathcal{C}) \sigma_R(\pi\lambda)^{\frac{1}{2}}/K_c\}. \quad (15)$$

This may be conveniently reduced to the simple form

$$[\mathcal{P}(\mathcal{C})]_{\alpha} = \mathcal{C}^{\frac{1}{2}} \{1 + \alpha M(\mathcal{C})\}, \quad (16)$$

where we define a normalised index of tempering

$$\alpha = \sigma_R(\pi\lambda)^{\frac{1}{2}}/K_c \quad (17)$$

and a normalised indentation load $\mathcal{P} = P/P_0$, the subscript zero relating to quantities measured in the untempered state ($\alpha=0$) such that

$$P_0 = (P/\mathcal{C}^{\frac{1}{2}})_0 = (P/c^{\frac{1}{2}})_0 \lambda^{\frac{1}{2}} = K_c L\lambda^{\frac{1}{2}}/\chi. \quad (18)$$

For a given tempering process, as characterised by the function $M(\mathcal{C})$, Equation (16) presents itself as a universal equilibrium relation in which absolute values are determined by three parameters: (i) P_0 determines the scale of loading, being in effect the force-necessary to drive the indentation crack through the distance λ in untempered plate, i.e. to $\mathcal{C} = 1$ [this parameter may be “calibrated” by direct measurement of the quantity $(P/c^{\frac{1}{2}})_0$]; (ii) λ itself determines the scale of the crack; (iii) α expresses the relative levels of the extrinsic (residual field) and intrinsic (surface tension) resistance to crack growth. We investigate the universal relations for both physically and chemically tempered plate below, noting that $d\mathcal{P}/d\mathcal{C} > 0$ represents stable equilibrium, $d\mathcal{P}/d\mathcal{C} < 0$ represents unstable equilibrium.

Physically tempered plate

With $M(c/d) = M(\mathcal{C})$ in Equation (5), our universal equilibrium relation becomes ($m_E = 1$)

$$[\mathcal{P}(\mathcal{C})]_{\alpha} = \mathcal{C}^{\frac{1}{2}} + \alpha(\mathcal{C} - 6\mathcal{C}^2/\pi + 3\mathcal{C}^3/4). \quad (19)$$

This function is plotted in Figure 7, for several values of α . It is noted that the curves corresponding to $\alpha=0$ (unstrengthened plate) corresponds to stable growth

†Either by direct application of Equation (1), substituting the appropriate component of P_L for $\sigma(0) dz$, or by the principle of geometrical similitude.

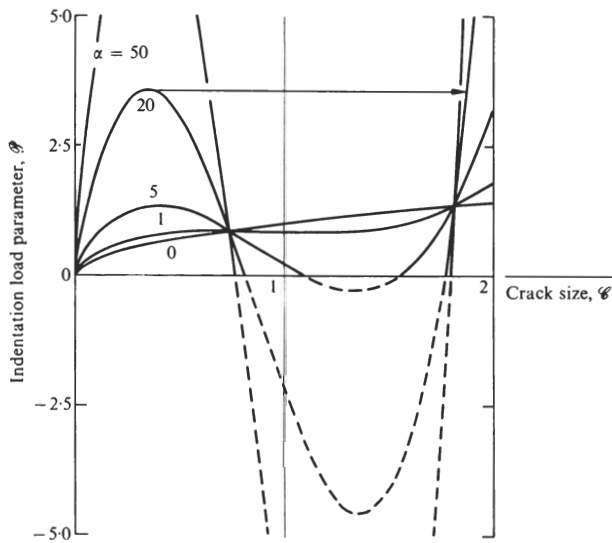


Figure 7. Universal equilibrium function $\mathcal{P}(\mathcal{C})$ for straight cracks in physically tempered plate. Curves shown for several degrees of tempering. Arrowed horizontal line indicates instability in crack propagation at $\alpha = 20$

throughout, with complete plate rupture at $\mathcal{C}=2$, $\mathcal{P}=\sqrt{2}$ (although edge effects will generally be manifest before this state is reached). The effect of strengthening, $\alpha > 0$, on the resistance to crack propagation is initially to increase this resistance (via the near compression zone), then to diminish it (via the central tension zone), and ultimately to increase it again (via the far compression zone). For sufficiently severe strengthening, $\alpha \gg 0$, this introduces certain instabilities into the fracture mechanics: in particular, the function $\mathcal{P}(\mathcal{C})$ passes through a well defined maximum, representing a change in the equilibrium from stable to unstable. Thus the effect of tempering may be seen as one of establishing a "macroscopic energy barrier" to the well developed indentation fracture (not unlike the barrier mentioned earlier in connection with the nucleation and formation of the crack, but this time on a considerably larger scale); once beyond the barrier, however, the crack accelerates rapidly at constant load (or, in a "fixed grips" arrangement, at constant outer displacement), thereby taking the plate to failure.†

Our quest for a failure condition therefore comes down to a straightforward determination of the maximum in the $\mathcal{P}(\mathcal{C})$ function. In what follows we shall designate any quantity evaluated at this maximum by asterisk notation. Putting $d\mathcal{P}/d\mathcal{C} = 0$ in Equation (19), the condition for extrema becomes

$$f(\mathcal{C}) = -1/\alpha \tag{20a}$$

where

$$f(\mathcal{C}) = 2\mathcal{C}^2(1 - 12\mathcal{C}/\pi + 9\mathcal{C}^2/4). \tag{20b}$$

†Note that for the more severely tempered plates the $\mathcal{P}(\mathcal{C})$ curves actually cross the \mathcal{C} axis within the central zone. In regions such as these it would be necessary to apply additional closure stresses to restrain crack extension, even if the external driving force were to be removed entirely subsequent to overcoming the energy barrier (as, perhaps, in an impact situation).

Solutions may be obtained graphically, as in Figure 8, from intersections between the two functions which comprise Equation (20). Variation in degree of tempering is conveniently represented by a shift in position of the horizontal broken line $-1/\alpha$ (≤ 0 , since $\alpha \geq 0$ always). For small α no intersections occur, i.e. the crack never becomes unstable. At first intersection, $f(0.922) = -1.168$, corresponding to $\alpha = 0.856$, the existence of an instability in the crack system is imminent. Upon increasing α above this transition value two intersections occur, the one at smaller \mathcal{C}

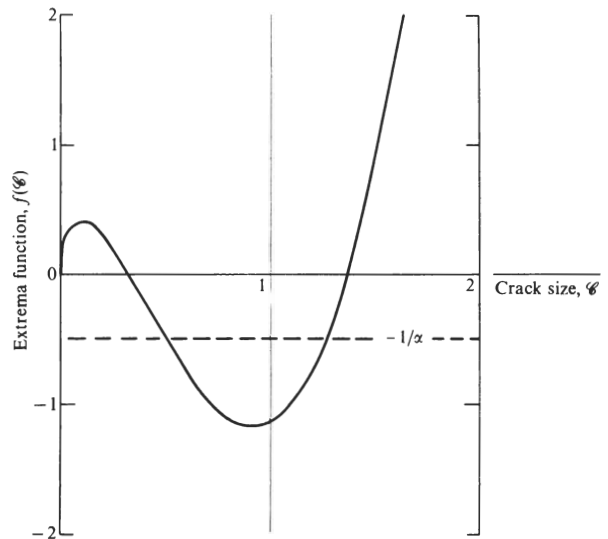


Figure 8. Graphical solution of Equation (20), for determining extrema in $\mathcal{P}(\mathcal{C})$ function for physically tempered plate

relating to the required maximum in \mathcal{P} and the other similarly to a minimum (see Figure 7). In the extreme of severe tempering, $\alpha \gg 0.856$, limiting intersections occur at $f(0.323) = 0 = f(1.374)$. Thus the critical crack penetration contracts within the range $0.922 > \mathcal{C}^* > 0.323$ as the degree of tempering increases within $0.856 < \alpha < \infty$: in particular, once the tempering exceeds moderate proportions (say, $\alpha > 20$) the location of the instability saturates rapidly at the limiting value of approximately one-sixth the plate thickness (i.e. well within the near-surface compression zone $0 < \mathcal{C} < 0.423$). Substituting this limiting value $\mathcal{C}^* = 0.323$ back into Equation (19) gives the corresponding limiting solution for the critical load,

$$\mathcal{P}^*(\alpha) = 0.568 + 0.149\alpha \approx 0.149\alpha, \quad (\alpha \gg 0.856). \tag{21}$$

Figure 9 compares the approximate form of this limiting solution with the exact solution evaluated numerically over the complete range of allowable α . Recalling that $\mathcal{P} = P/P_0$, $\lambda = d$, recourse to Equations (17) and (18) enables us to express the critical load in absolute terms:

$$P^* \approx 0.264 \sigma_R dL/\chi, \quad (\alpha \gg 0.856). \tag{22}$$

This result has some interesting implications. In its limiting form, the critical load function is entirely

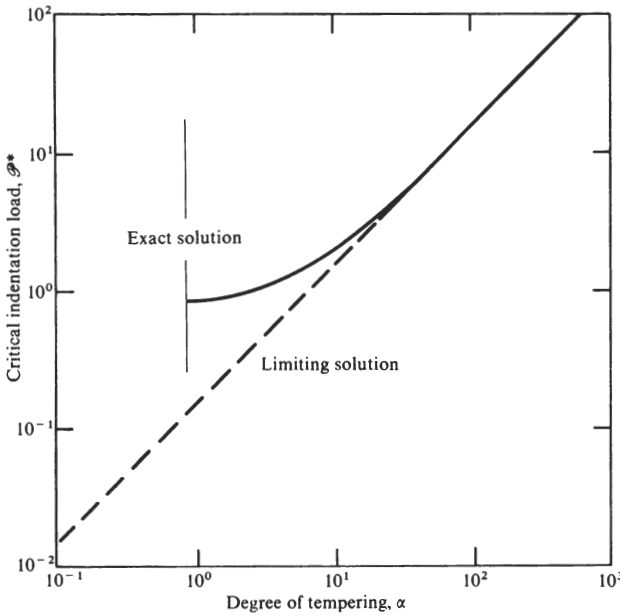


Figure 9. Comparison of exact and limiting solutions for normalised indentation load, \mathcal{P}^* , at instability as function of degree of tempering, α , for physically tempered plate. Note nonexistence of instability at $\alpha < 0.856$

independent of material constants. While this may at first seem surprising, reference to the earlier Equation (15) shows that for $\alpha \gg 0.856$ the intrinsic term $K_c [\ll 1.168 \sigma_R (\pi \lambda)^{\frac{1}{2}}]$ tends to cancel out; and it is only through K_c that material constants can enter the formulation; see Equation (9). We shall elaborate further on this point in the Discussion. Extrinsic parameters relating to the residual field, σ_R and d , and to the contact configuration, χ , control the instability. We may note, however, the absence of any extrinsic parameters relating to flaw characteristics, reflecting on the fact that the crack is well developed at critical loading.

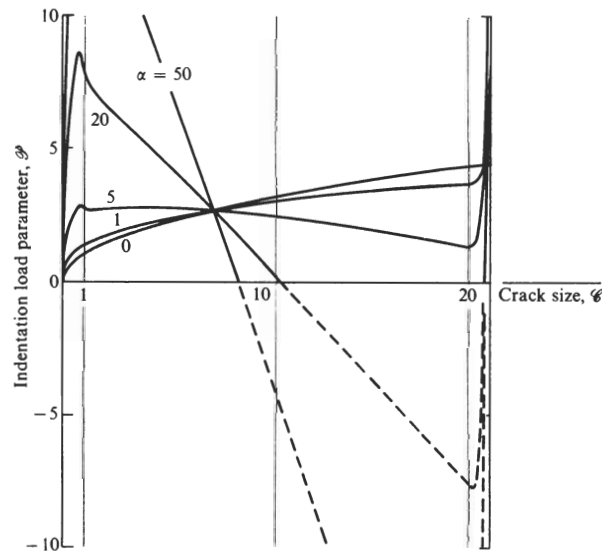


Figure 10. Universal equilibrium function, $\mathcal{P}(C)$, for straight cracks in chemically tempered plate. Curves shown for several values of α , at $\Delta = 0.1$

Chemically tempered plate

Proceeding as for physically tempered plate, we insert $M(c/\delta, \delta/d) = [M(C)]_{\Delta}$ from Equations (8), with $\Delta = \delta/d$, into Equation (16) to obtain the universal equilibrium function $[\mathcal{P}(C)]_{\alpha, \Delta}$ for chemically tempered plate. Plots of this function are given for various values of α (Δ fixed) in Figure 10 and of Δ (α fixed) in Figure 11 ($m_E = 1$). The curves are seen to have the same general features concerning extrema as the analogous curves of Figure 7. In particular, the location of the instability again saturates rapidly at a limiting crack penetration well within the near surface compression zone. Then the function $[M(C)]_{\Delta} = M(C)$ in Equation (8a) is the appropriate one to adopt in any evaluation of the maximum in the equilibrium equation:

$$[\mathcal{P}(C)]_{\alpha} = C^{\frac{1}{2}} + \alpha(C - 2C^2/\pi), \quad (0 \leq C \leq 1). \quad (23)$$

Accordingly, the condition for extrema, $d\mathcal{P}/dC = 0$, becomes, in the same way as before,

$$f(C) = -1/\alpha \quad (24a)$$

where

$$f(C) = 2C^{\frac{1}{2}}(1 - 4C/\pi). \quad (24b)$$

Graphical solutions, Figure 12, indicate the critical crack penetration to contract within the range $1 < C^* > 0.785$ † as the degree of tempering increases within $1.830 < \alpha < \infty$. Thus, inserting the limiting value $C^* = 0.785$ for infinitely severe tempering back into Equation (23), we have the corresponding limiting solution for the critical indentation load,

$$\mathcal{P}^*(\alpha) = 0.886 + 0.393\alpha \approx 0.393\alpha, \quad (\alpha \gg 1.830). \quad (25)$$

A comparison plot between this limiting solution, in its approximate form, and the exact solution over the allowable range of α is given in Figure 13. An absolute expression for the critical load follows, from Equations

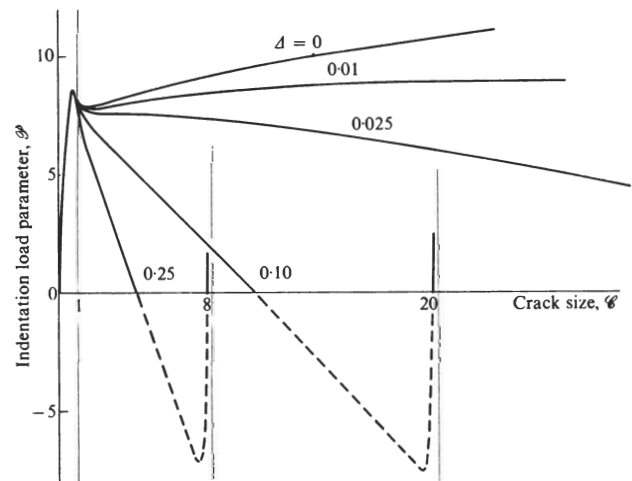


Figure 11. Universal equilibrium function, $\mathcal{P}(C)$, for straight cracks in chemically tempered plate. Curves shown for several values of Δ , at $\alpha = 20$. Note invariance of plot in near compression zone $0 \leq C \leq 1$

†For thick plates (depth of chemical layer invariant), a weak, secondary maximum may occur at $C^* > 1$ (see curves at small d , Figure 11).

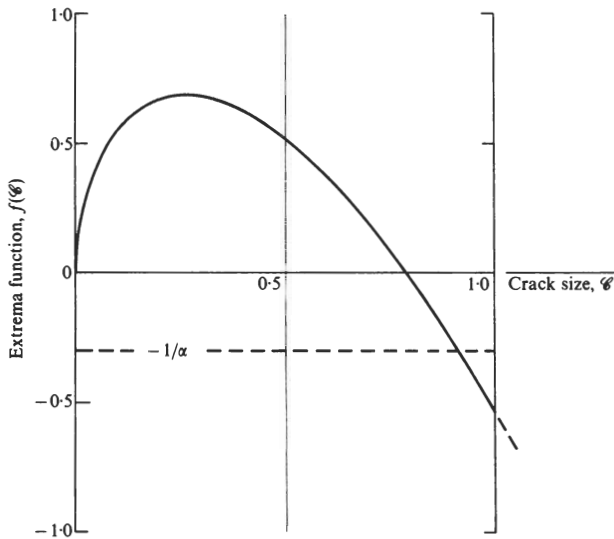


Figure 12. Graphical solution of Equation (24), for determining extrema in $\mathcal{P}(\phi)$ function for chemically tempered plate

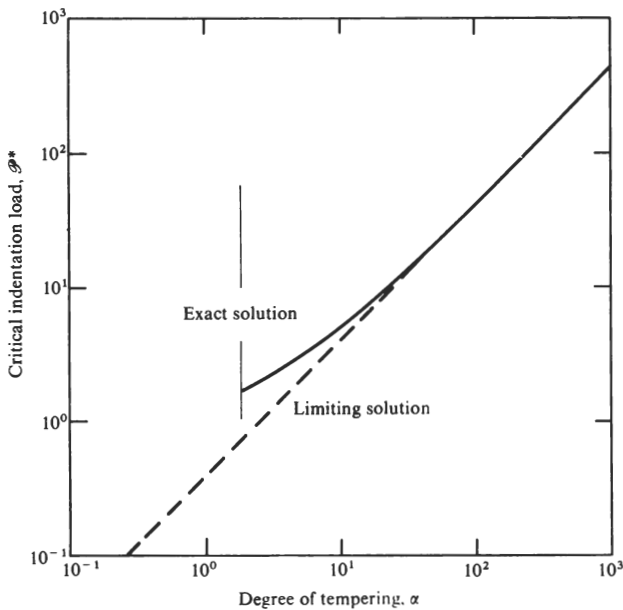


Figure 13. Comparison of exact and limiting solutions for normalised indentation load, \mathcal{P}^* , at instability as function of degree of tempering, α , for chemically tempered plate. Note nonexistence of instability at $\alpha < 1.830$

(17) and (18) and $\mathcal{P} = P/P_0$, $\lambda = \delta$:

$$P^* \approx 0.697 \sigma_R \delta L / \chi, (\alpha \gg 1.830), \quad (26)$$

in analogy with Equation (22).

Once more we may note the independence of the critical load function on intrinsic material parameters and flaw characteristics.

More general contact situations

“POINT CONTACT” LOADING—DISTORTION OF “PENNY LIKE” CRACKS IN RESIDUAL FIELDS

In the above treatment we have somewhat idealised our crack system. Apart from approximations in the

fracture mechanics analysis, we have the simplistic physical picture of an indentation mode of failure in which a contact-induced crack advances stably through a contact compression layer toward a well defined instability point, with critical extension occurring uniformly along the entire front. Now in most real contact (especially impact) situations, the geometrical conditions of fracture are likely to be considerably more complex than this. In what significant ways, if any, might we expect such geometrical complexities to affect the above expressions, notably Equations (22) and (26), for the contact fracture resistance?

Most generally, indentation cracks will tend to be of the “point contact” rather than “line contact” type. Even a linear scratch made with a translating particle should strictly, in the context of contact-induced failure, be viewed as the trace of a fracture pattern which, at any given instant, corresponds essentially to a configuration of point contact loading (although if the indenting particle were to be removed prior to failure, and the remnant crack were to extend under the subsequent action of incremental driving forces, the line approximation would be appropriate). In their well developed form, contact cracks produced by point forces in otherwise stress-free plates tend to a “penny like” geometry (i.e. they assume a near-circular extension front), regardless of the nature of the indenter:⁽²⁰⁾ “blunt” indenters (e.g. spheres)

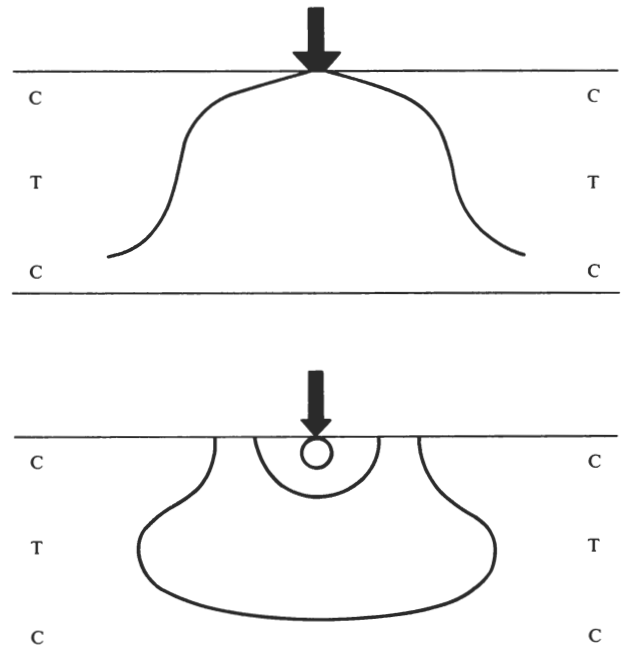


Figure 14. Schematic section views of Hertzian crack (top: “blunt” indenters) and median crack (bottom: “sharp” indenters) evolution in point contact loading. C. compression zone; T. tension zone

produce the Hertzian cone cracks already mentioned; “sharp” indenters (e.g. pyramids, cones) produce “median” cracks, half-penny configurations with contact point as centre and load axis as diagonal. It is here that the major obstacle to a general analysis of tempered plate failure arises. Quite apart from the

difficulty of computing stress intensity factors in such cases, the superposed residual stress field will act to disturb the regular geometry of the cracks.

However, for the level of fracture mechanics treatment aimed at here it is not necessary to undertake a full-scale, three dimensional stress trajectory analysis of prospective crack paths^(8, 10) in the combined indentation and residual fields. A few qualitative remarks, based partly on some visual observations,⁽¹¹⁾ but mainly on the knowledge that brittle fractures tend to seek an orientation which maximises the tensile loading, with equilibration of driving forces everywhere along the crack front, will suffice.⁽¹³⁾

Figure 14 accordingly indicates the geometrical evolution of equilibrium contact cracks for the extremes of blunt and sharp indenters. Taking the Hertzian configuration first, we may expect the crack initiated as a cone to take on the appearance of a bell as it traverses the plate: the outer compressive stresses will tend to make the crack surface more shallow, the inner tensile stresses correspondingly to make the surface more steep (the front remaining essentially circular). Ultimately, the crack will tend to flare out laterally as it approaches the far surface layer, and thence spread through the plate.

As for the median configuration, the crack initiated as a half-penny will tend to extend preferentially into the central tensile zone at a point directly below the contact, and thereafter develop along a continuously distorting front (the crack plane remaining unchanged). Again, the crack, once beyond the near surface compression layer, becomes free to propagate laterally within the inner confines of the plate.

The geometrical complexity of the equilibrium indentation cracks represented schematically in Figure 14, compounded by dynamic processes (notably bifurcation) once a critical penetration is exceeded, would appear to rule out any possibility of a general stress intensity factor determination. However, we are concerned primarily with events immediately prior to instability, which may occur well within the near surface compression zone (recall that this is so for straight cracks); in such favourable cases the distortion in crack pattern may be regarded as minimal over the propagation range of interest. We shall accordingly proceed on the assumption that the essential penny like character of the point-contact cracks remains intact over this range.

FRACTURE MECHANICS AND UNIVERSAL FAILURE RELATIONS FOR POINT CONTACT LOADING

We attempt now to develop a general fracture mechanics formulation for penny like cracks in tempered plate, retaining the essential elements of the simplistic straight crack model. In line with the implications of Equations (22) and (26), we may anticipate characteristic parameters of the residual field, representing both intensity (σ_R) and spatial extent (λ), and of the contact configuration (χ), to play a key role in the failure mechanism.

Stress intensity factors—dimensional analysis

We have already alluded to the difficulty in computing stress intensity factors for complex crack configurations. In seeking an appropriate expression for extension through the combined residual and bearing fields analogous to that of Equation (14), formulae need to be obtained for the components K_R and K_B . It turns out that the formidable prospect of a first principles analysis can be conveniently circumvented here by making use of the geometrical similarity of well-developed penny like cracks, adopting a dimensional argument to determine each of the two components separately.

Let us start with the residual stress intensity factor. Since the surface compressive stress $-\sigma_R$ uniquely determines the intensity of the residual field, e.g. Equations (2) and (6), it may immediately be inferred that $K_R \propto -\sigma_R$. Again, since the characteristic crack dimension c uniquely determines the spatial extent of fracture for a geometrically similar system, the dimensional form of the stress intensity factor requires that $K_R \propto c^{\frac{1}{2}}$. Now if the field were to be homogeneous, incorporation of a dimensionless, edge effect term $m_E = m_E(c/d)$ would exhaust the remaining independent variables. Then to allow for an inhomogeneous field, whose gradient is uniquely determined by the characteristic dimension λ , it becomes a simple matter of incorporating a further dimensionless term $m_R = m_R(c/\lambda)$. We may therefore write generally, for a given plate,

$$K_R(c) = -m_E m_R \sigma_R (\pi c)^{\frac{1}{2}} = -M(\mathcal{C}) \sigma_R (\pi \lambda)^{\frac{1}{2}} = K_R(\mathcal{C}), \tag{27}$$

in accordance with our earlier, reduced notation. The form of K_R in this expression is seen to be essentially the same as that in Equations (4), (7), and (14) for straight cracks.

Now let us turn to the bearing stress intensity factor. In this case the intensity of the stress field is determined by the point load divided by a characteristic support area (taken as area of the surface everywhere distant c from the contact), so that $K_B \propto P/c^2$. (This term automatically allows for inhomogeneity in the field.) The factor representing the spatial extent of fracture must remain unchanged, i.e. $K_B \propto c^{\frac{1}{2}}$, since it is the same crack that is being subjected to the two fields. This leaves only an indentation geometry term χ (which automatically allows for edge effects) to be incorporated. Our general stress intensity factor for point contact indenters becomes

$$K_B(c) = \chi P/c^{3/2} = \chi P/\lambda^{3/2} \mathcal{C}^{3/2} = K_B(\mathcal{C}). \tag{28}$$

Thus, with the indentation field the form of K_B differs slightly from that in Equations (13) and (14) for straight cracks.† A more rigorous derivation of Equation (28) is given elsewhere.⁽²⁰⁾

†This comes about as a result of replacing Lc (line contact cracks) by c^2 (point contact cracks) as the support area for the indentation load.

The composite stress intensity factor may therefore be written

$$K(\mathcal{C}) = \chi P/\lambda^{3/2}\mathcal{C}^{3/2} - M(\mathcal{C})\sigma_R(\pi\lambda)^{\frac{1}{2}}. \quad (29)$$

As with the analogous Equation (14), this expression provides a basic starting point for a complete fracture mechanics analysis.

Equilibrium cracks and critical indentation relations

Combining Equation (9) with Equation (29) gives an equilibrium relation for the indentation cracks:

$$\chi P/K_c\lambda^{3/2} = \mathcal{C}^{3/2}\{1 + M(\mathcal{C})\sigma_R(\pi\lambda)^{\frac{1}{2}}/K_c\}. \quad (30)$$

This may be reduced to

$$[\mathcal{P}(\mathcal{C})]_{\alpha} = \mathcal{C}^{3/2}\{1 + \alpha M(\mathcal{C})\}, \quad (31)$$

where α is a normalised index of tempering as previously defined, and $\mathcal{P} = P/P_0$ is a normalised indentation load such that

$$P_0 = (P/\mathcal{C}^{3/2})_0 = (P/c^{3/2})_0\lambda^{3/2} = K_c\lambda^{3/2}/\chi, \quad (32)$$

the subscript zero indicating quantities measured in the untempered state. Equation (31) is our universal equilibrium relation for point contact loading, in which the dimensionless function $M(\mathcal{C})$ characterises the tempering process.

Then as long as the equilibrium function $\mathcal{P}(\mathcal{C})$ has a well defined maximum, such that failure may be associated with a critical crack penetration \mathcal{C}^* and corresponding residual-field function $M(\mathcal{C}^*) = M^*$, Equation (31) provides an explicit expression for the critical load in terms of degree of tempering. In the limit of severe tempering we obtain

$$\mathcal{P}^*(\alpha) = \mathcal{C}^{*3/2}(1 + M^*\alpha) \approx \mathcal{C}^{*3/2}M^*\alpha, \quad (\alpha \gg 1/M^*). \quad (33)$$

Combination with Equations (17) and (32) gives the critical load in absolute terms;

$$P^* \approx \text{const. } \sigma_R\lambda^2/\chi, \quad (\text{point contact; } \alpha \gg 1/M^*). \quad (34)$$

This compares with the corresponding result for straight cracks, Equations (22) and (26);

$$P^* \approx \text{const. } \sigma_R\lambda L/\chi, \quad (\text{line contact; } \alpha \gg 1). \quad (35)$$

Thus, despite considerable uncertainty in the details of the $\mathcal{P}(\mathcal{C})$ functions for given tempered plates, we have been able to determine the essential form of the failure relations for basic indentation fracture systems. It is only the constants of proportionality in Equations (34) and (35) which depend on such details. Equations (22) and (26) indicate these constants to be of order unity; for a more exact evaluation than this one might consider resorting to computer techniques (using finite element analysis, say), but direct experimental calibration (with plates and indenters whose characteristics have been independently determined) would perhaps be simpler. Once more we may note the absence of any material or flaw parameters in the limiting failure relations.

Notwithstanding the need for experimental verification of the above results, we might feel justified in

seeking an order of magnitude estimate of a typical load to failure. Referring to Equation (34), we insert the following values for Vickers diamond pyramid indentation on physically tempered glass plate: const. ≈ 1 ; $\sigma_R \approx 100$ MPa and $\lambda = d \approx 3$ mm; $\chi = K_c/(P/c^{3/2})_0 \approx 5 \times 10^5 \text{ N m}^{-3/2}/1 \times 10^7 \text{ N m}^{-3/2} \approx 0.05^{(20)}$. This gives $P^* \approx 2 \times 10^4$ N, a substantial load in conventional indentation fracture testing.⁽¹⁰⁾

Discussion

We have derived simple relations for the critical load to contact failure in tempered glass plates. Our analysis has been based on several assumptions and idealisations; these, however, bear chiefly on the proportionality constants in the critical relations. The extreme range of conditions covered, from line contact to point contact loading, straight crack to penny crack geometry, blunt to sharp indenters, etc., should embrace most real contact situations. Although exclusive consideration has been given to static crack systems (or quasistatic systems where kinetic effects have been involved), the analysis may be readily extended to include certain well defined impact situations: provided the contact velocity, v , does not approach the velocity of elastic waves in the system, knowledge of the static contact force/displacement behaviour permits a unique determination of the function $P(v)^{(22)}$ (the incursion of dynamic terms at high contact velocities invalidating this procedure), hence a critical velocity v^* .

Of particular interest are the results in the limit of severe tempering. For a given indenter it is the residual-field parameters σ_R and λ in Equations (34) and (35) which control the resistance to contact failure. It will be recalled that the critical penetration corresponding to instability in the well developed fracture system tends to fall within the near surface compression zone: this leads to the limiting picture of crack evolution in terms of a balance between two dominant forces, in which the indentation field alone drives the crack and the residual field alone resists it. With the intrinsic surface tension term insignificant in the balance of forces, knowledge of the physical properties of the test material is unnecessary.† So also is knowledge of the flaw statistics, provided the material is sufficiently brittle (as most silicate glasses usually are) under the operative test conditions that the energy barrier to ultimate instability of the crack greatly exceeds that to initiation.

In this same context of limiting behaviour, even gross uncertainty as to the correct form of the condition for crack propagation has little bearing on the results. We have taken the equilibrium condition $K = K_c$, as per Equation (9), as our basis for predicting the onset of plate failure, throughout the above analysis. Others might contend that a more correct condition for failure should be $K = K_b \approx 4K_c^{(23, 24)}$ with K_b corresponding to the stress intensity factor

†Of course, it is appreciated that mechanical, thermal and chemical properties must be instrumental in determining the residual-stress profile for any given tempering process in the first place.

at which branching occurs, since catastrophic breakdown of the plate certainly does involve a fragmentation mode. However, replacement of K_c by K_b in Equations (15) and (30) would lead to precisely the same limiting results as before: either term is negligible in comparison with the residual-field term $\sigma_R(\pi\lambda)^{1/2}$ in these equations, and hence cancels. Similarly, the influence of kinetic crack growth, as per Equation (10), must be expected to be infinitesimal: this is because the range of crack penetrations over which the condition $0 \leq K < K_c$ (the maximum range of stress intensity factors over which subcritical extension can occur) is satisfied, at a given indentation load, itself becomes infinitesimal in the severe tempering limit. (That is, for $\sigma_R(\pi\lambda)^{1/2} \gg K_c$ in Equations (14) and (29), small changes $\Delta\mathcal{E}$ correspond to large changes $\Delta K > K_c$.) These remarks apply not only to indentation-induced failure, but also to spontaneous failure from remnant cracks as outlined in an earlier section of the paper: thus we may note in Figure 3 how an increased degree of tempering for physically tempered plate, as represented by the sequence $1 \rightarrow 2 \rightarrow 3 \rightarrow$, diminishes the range of crack penetrations over which the condition $0 \leq K < K_c$ prevails.

Of course, for real contact situations the limiting failure relations can provide no more than first approximations to the critical load. The error incurred in extrapolating these relations back to low degrees of tempering may be gauged from Figures 9 and 13. To illustrate, let us investigate the prospective error for typical strengthened glass plate using values previously quoted for the relevant parameters: with $K_c \approx 5 \times 10^5 \text{ Nm}^{-3/2}$, $\sigma_R \approx 100 \text{ MPa}$, and $\lambda = d \approx 3 \text{ mm}$ (physical tempering) or $\sigma_R \approx 1000 \text{ MPa}$ and $\lambda = \delta \approx 0.1 \text{ mm}$ (chemical tempering), Equation (17) gives $\alpha \approx 20-30$, which is seen to correspond to an error of less than 20%. At lower values of α the discrepancy rapidly increases, as the contribution of the intrinsic surface tension term makes itself felt in the overall fracture resistance. However, in this region the whole concept of failure instability becomes less well defined, and cracks are more prone to arrest without ever achieving a fragmentation configuration.

There remains the issue of flexural effects in the plate failure process. As mentioned in the introduction, such effects are likely to cause a transition to a "catastrophic flaw" mode of failure as plate thickness diminishes.⁽⁷⁾ (A similar transition may be envisaged as indenter bluntness and softness increase, in terms of an enhanced initiation barrier to contact fracture.) Ultimately, therefore, optimum strength design calls for a complete description of both modes. In this connection it is interesting to reflect that a change in strengthening procedure (e.g. in going from physical to chemical tempering) which raises the resistance to failure in the catastrophic flaw mode (by virtue of increasing σ_R) might well lower the resistance in the indentation crack mode (by virtue of decreasing λ). Standardised safety tests for tempered glass objects, generally being concerned more with simulating service conditions than with elucidating the physical processes of failure themselves, rarely consider such

factors in the evaluation of strength characteristics: the testing of strengthened spectacle lenses (e.g. ball drop test, ballistic missile test)⁽²⁵⁾ is just one example in which data obtained is of little or no use in predicting behaviour under alternative contact situations.

Even in cases where the indentation crack mode of failure is known always to prevail, flexural effects can be important. For a start, since the indentation crack initiates on the compression side of a bent plate, an additional closure term should be added to the crack-force balance equation. Thus, in analogy with Equations (27) and (28), one obtains a flexure stress intensity factor for a centrally loaded circular plate,⁽²⁶⁾ $K_F = -m_E m_F (P/d^2)(\pi c)^{1/2}$, where m_F incorporates details of the specimen support and the remaining terms have their previous meaning. Addition of this component to the composite stress intensity factor, Equation (29), would clearly lead to increased P^* in equation (34). Again, the partition of energy delivered by the loading system into the indentation and flexure fields will inevitably increase the work to failure: for a fixed energy system (e.g. impact particle of fixed velocity) this will lead to a diminished contact load. Seen in this light, the results of the present analysis derived in the zero flexure approximation serve as a conservative basis for design against indentation-induced failure.

Acknowledgements

Thanks are due to V. R. Howes and M. M. Lang for discussions in the initial stages of this work. Funding through the Australian Research Grants Committee is acknowledged.

References

1. Griffith, A. A. (1920). *Phil. Trans. R. Soc.* **A211**, 163.
2. Olcott, J. S. (1963). *Science* **140**, 1189.
3. Stookey, S. D. (1965). In *High Strength materials*, Ed. V. F. Zackay. Wiley, New York. P. 669.
4. Ernsberger, F. M. (1966). *Glass Ind.* **47**, 422.
5. Zijlstra, A. L. & Burggraaf, A. J. (1968-9). *J. Non-Cryst. Solids* **1**, 49, 163.
6. Littleton, J. T. & Preston, F. W. (1929). *J. Soc. Glass Technol.* **13**, 336.
7. Glathart, J. L. & Preston, F. W. (1968). *Glass Technol.* **9**, 89.
8. Frank, F. C. & Lawn, B. R. (1967). *Proc. R. Soc. Lond.* **A299**, 291.
9. Lawn, B. R. & Swain, M. V. (1975). *J. mater. Sci.* **10**, 113.
11. Aclouque, P. (1965). In *Symposium on mechanical strength of glass and ways of improving it*. Union Scientifique Continentale du Verre, Charleroi, Belgium. P. 851.
12. Barsom, J. M. (1968). *J. Am. Ceram. Soc.* **51**, 75.
13. Lawn, B. R. & Wilshaw, T. R. (1975). *Fracture of brittle solids*. Cambridge University Press, Cambridge. Chs. 2, 3, 4 and 8.
14. Paris, P. C. & Sih, G. C. (1965). In *Fracture toughness testing and its applications*. A.S.T.M. Spec. Tech. Publ. **381**, P. 30.
15. Bartenev, G. M. (1949). *Zh. tekh. Fiz.* **19**, 1423.
16. Gardon, R. (1965). In *Proceedings of the seventh International Congress on Glass*. International Commission on Glass, Charleroi, Belgium. Paper 79.
17. Nordberg, M. E., Mochel, E. L., Garfinkel, H. M. & Olcott, J. S. (1964). *J. Am. Ceram. Soc.* **47**, 215.
18. Wiederhorn, S. M. (1967). *J. Am. Ceram. Soc.* **50**, 407.
19. Wiederhorn, S. M. (1969). *J. Am. Ceram. Soc.* **52**, 99.
20. Lawn, B. R. & Fuller, E. R. (1975). *J. mater. Sci.* **10**, 2016.
21. Swain, M. V. & Lawn, B. R. *Int. J. Rock Mech.* In press.
22. Wiederhorn, S. M. & Lawn, B. R., to be published.
23. Congleton, J. & Petch, N. J. (1967). *Phil. Mag.* **16**, 749.
24. Kerkhof, F. & Richter, H. (1969). In *Proceedings of Second International Conference on Fracture*. Chapman & Hall, London. Paper 40.
25. Wigglesworth, E. C. (1972). *Am. J. Optom.* **49**, 287.
26. Evans, A. G. & Davidge, R. W. (1971). *Glass Technol.* **12**, 148.